RSC Advances

ROYAL SOCIETY OF CHEMISTRY

www.rsc.org/advances

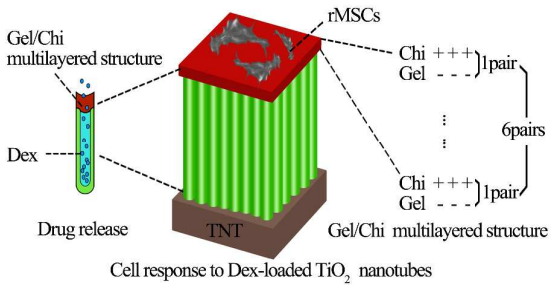

Schematic illustration of cellular responses of rMSCs to Dex-loaded TNT arrays.

RSC Advances

RSCPublishing

PAPER

Influence of Dexamethasone-loaded TNTs on the Proliferation and Osteogenic Differentiation of Rat Mesenchymal Stem Cells

Cite this: DOI: 10.1039/x0xx00000x

Sheng Yang,‡[a] Ming Wang,‡[a] He Zhang,[a] Kai-yong Cai,[b] Xin-kun Shen,[b] Feng Deng,[a] Yi Zhang[a] and Lu Wang*[a]

Received 30th September 2014,
Accepted 00th January 2014

DOI: 10.1039/x0xx00000x

www.rsc.org/advances

The main cause of titanium implant failure is inferior osseointegration. Dexamethasone (Dex), a potent synthetic member of the glucocorticoid class of steroid drugs, has been widely used due to its potential for inducing osteogenic differentiation of stem cells. In this study, a controlled-release Dex nanocarrier was successfully established by combining titanium nanotubes (TNTs) with self-assembly multilayer gelatin/chitosan (Gel/Chi). The surface characteristics with three different diameter TNTs were investigated by scanning electron microscopy (SEM), contact angle measurement, X-ray fluorescence spectrometer (XRF) and Fourier transform infrared spectrometry (FTIR) and denoted as 30nm/Dex/$(Gel/Chi)_6$, 70nm/Dex/$(Gel/Chi)_6$, and 100nm/Dex/$(Gel/Chi)_6$. During the 14-day drug release assay, Dex released from TNTs demonstrated an initial burst phase followed by a sustained stage. Mesenchymal stem cells isolated from Sprague–Dawley rat bone marrow (rMSCs) and cultured on all substrate surfaces were observed by confocal laser scanning microscopy (CLSM) and SEM. MTT assay showed greater cell adherence and proliferation abilities compared with smooth titanium, especially on 70nm/Dex/$(Gel/Chi)_6$. rMSCs on 30nm/Dex/$(Gel/Chi)_6$ delineated the highest alkaline phosphatase activity and mineralization levels, as well as gene expression of Runt-related transcription factor 2 (Runx2) and Osterix (OSX) compared with smooth titanium. Above all, the Dex-loaded TNTs were able to promote adherence, proliferation, and osteogenic differentiation of rMSCs. This innovative method may have potential value for constructing titanium implants to accelerate bone integration and improve therapeutic success rates.

Introduction

Although implant biomaterials based on pure titanium have been widely utilized for orthopedic treatment and have already achieved a relatively high success rate, many cases still fail because of inferior osseointegration or peri-implantitis.[1-3] Osseointegration is the direct interface between alloplastic material and bone, in which the stem cells play essential roles in responding to the material surface and then being triggered to differentiate into osteogenic cells. In order to maintain these natural actions, many scholars have developed different methods, such as biofunctional material coatings,[4] chemical composition adjustments,[5] topological structure control,[2] etc. According to the natural features of the architecture and the multiple related components of bone, the ideal approach should maintain a cost-effective and flexible framework, mimic the physiological microenvironment of bone cells, and provide nanotopography on implant surfaces.[6] Nano-construction on the surfaces of metal implants that will aid in the delivery/release anti-inflammatory drugs or osteogenesis factors to the vicinity of the implants is currently being explored.

Previous studies demonstrated that nanoscale materials clearly promoted both cell proliferation and osteogenic differentiation, especially titanium dioxide nanotubes (TNTs); these TNTs have shown unparalleled advantages and attracted considerable attention for their applications in biomaterial science and technology.[7-9] TNTs have displayed favorable biocompatibility and no immunogenicity because of their attractive surface properties, including increased hydrophilia,[10] suitable roughness,[11] and higher surface-to-volume ratio.[12,13] The nanotopographic features of TNTs have proven suitable for mesenchymal stem cell (MSC) proliferation and osteogenic differentiation. As TNTs are hollow and can be filled with different molecules, such as bioactive polypeptides, nucleic

[a]*Chongqing Key Laboratory of Oral Diseases and Biomedical Sciences, College of Stomatology, Chongqing Medical University, Chongqing 401147, China*
[b]*Key Laboratory of Biorheological Science and Technology, the Ministry of Education, College of Bioengineering, Chongqing University, Chongqing 400044, China*
‡ *Both authors contributed equally to this work.*
**Corresponding author.*
Tel: (+008623) 8886 0085, (+0086) 136 1828 8326.
E-mail addresses: wanglu19631013@163.com.

acids, and chemicals, various types of drug delivery or controlled release systems using TNTs have been explored.[12,14] One of the most effective osteogenesis proteins, recombined human bone morphogenetic protein 2 (rhBMP2), has been successfully loaded into TNTs; however, this strategy would be potentially expensive and problems, such as denaturation when exposed to physiological environments[15] and serious inflammation and allergy.[16]

Dexamethasone (Dex) demonstrates the significant characteristic of promoting the osteogenic differentiation of bone marrow mesenchymal stem cells.[17,18] For example, human MSCs cultured in blended nanofibers with Dex via coaxial electrospinning showed higher alkaline phosphatase (ALP) expression and calcium deposition in vitro.[19] Nanoparticles, such as poly (lactic-co-glycolic acid) and carboxymethylchitosan/poly(amidoamine) polymers conjugated with Dex have also been demonstrated to effectively direct MSCs osteogenic differentiation.[20]

To use TNTs as drug delivery vehicles for sustained release, we need to construct biomaterial "lids" for them in order to avoid a severe loss of biomolecules during initial administration. For instance, gelatin (Gel, polyanionic) and chitosan (Chi, polycationic), as natural polymers, are the best options according to their excellent biocompatibility and biodegradability.[15,21-23] These natural polymers also possess abundant ligands for cell attachment that provide opportunities for functionalization and formation of cell binding islands. Gel/Chi materials not only demonstrate prominent protein/extracellular matrix (ECM) adsorption capacity and cytocompatibility, but also mimic the structures and biofunctions of osteogenesis ECM in vivo.[24] A Gel/Chi aggregation layer forms mesoporous ultramicrostructures for osteoblasts which acts as a fertilized breeding ground that allows for exchange of nutrition and metabolism during cell growth.[25,26] Therefore, we hypothesized that Gel/Chi is a feasible material to seal Dex into TNTs and deliver Dex in a controlled manner.

In this study, our aim was to combine both TNTs and Dex advantages to solve the aforementioned problems. We fabricated vertically aligned TNTs on titanium substrates by electrochemical anodic oxidation, then successfully loaded Dex into TNTs with Gel/Chi self-assembly "lids" to form a controlled drug release system. Sprague-Dawley rat MSCs (rMSCs) were used to evaluate the characteristics and biological properties of these structures. The use of this novel method will allow the creation of drug-loaded titanium implants for further biomedical applications.

Experimental section

Materials

Ti foil (0.25 mm thickness, 99.5% purity) was purchased from Alfa Aesar Co (China). Chitosan (CAS: 9012-76-4) and gelatin (CAS: RN 9000-70-8) were both provided by Sigma-Aldrich (USA). Dexamethasone (CAS: 50-02-2) was purchased from J&K Scientific (Germany). MTT cell proliferation and cytotoxicity assay kit (Cat No: C0009) and BCA protein assay kit (Cat No: P0012) were both purchased from Beyotime Co (China). Alkaline phosphatase (AKP/ALP) kit (Cat No: A059-2) was provided by Nanjing Jiancheng Bioengineering Institute (China). Alizarin Red S staining kit (Cat No: 0223) was provided by ScienCell Research Laboratories (USA). RNAiso plus (Code No: 9108/9109), PrimeScript RT reagent kit with gDNA eraser (Code No: RR820A) and Real-Time PCR assay kit (Code No: RR047A) were all purchased from Takara (Japan).

Fabrication of TNTs

The electrochemical anodic oxidation method was applied to prepare the TNTs.[14] Ti foil was cut into 1cm×1cm sizes and washed with 75% ethanol, acetone, isopropanol, 75% ethanol, and distilled water, respectively, by sonication for 15 min each. The foil pieces were then dehydrated using nitrogen gas. A solution compound based on glycerol and water (1:1, v/v) containing 0.27 M NH4F was used as the electrolyte. Anodization was conducted at a constant voltage of 10v, 20v, and 30v for 3h to prepare 30nm, 70nm, and 100nm diameter TNTs, respectively, with Ti foil as the anode and Pt foil as cathode. Ti substrates with TNTs were thoroughly rinsed with a large amount of distilled water and then dried using nitrogen gas.

Drug loading

A 5mg/ml Dex solution was prepared with distilled water. In total, 40µl of this solution was dropped onto each TiO_2 nanotube substrate,[15,27] and the samples were allowed to dry at room temperature for 6h.

Multilayered coatings of Dex-loaded TNTs

A polymer solution of Gel was prepared at a concentration of 10 mg/ml with phosphate buffered saline (PBS), and a Chi solution of 10 mg/ml was prepared with 0.3% (v/v) acetic acid. Exactly 100µl of the prepared Gel solution was pipetted onto the surfaces of 30nm, 70nm, and 100nm diameter TNTs which had been previously loaded with Dex. Then, the samples were rotated at 4000rpm for 40s with a spin coater. The samples were subsequently washed with ultrapure water, and then 100µl of the Chi solution was doped onto the precoated samples. The samples were subsequently rotated and washed in the same manner as the Gel samples. The above procedure was repeated another 5 times so that there were 6 cycles of Gel and Chi coatings performed on each nanotube substrate (Gel+Chi coating is assumed as one cycle. One cycle means two layers, gel coating layer and chi coating layer.). The samples were denoted as 30nm/Dex/$(Gel/Chi)_6$, 70nm/Dex/$(Gel/Chi)_6$, and 100nm/Dex/$(Gel/Chi)_6$.

Surface characterization

Structural characterizations of the fabricated TNTs with multilayer coating were imaged with a field emission scanning electron microscope (FEINova 400 Nano SEM, Phillips Co, Holland). The chemical composition of the substrates was detected with an X-ray Fluorescence Spectrometer (XRF-1800, Shimadzu Co., Japan). The contact angles of Ti and 30nm, 70nm, and 100nm diameter TNTs with different layer coatings were measured using a contact angle measuring apparatus (HARKE-SPCA, Beijing, China). A distilled water droplet of 5µl was used for each measurement and exposed for 15s at room temperature. Five replicates were performed in each group. The final result was the mean value for each sample. FTIR analysis was performed to demonstrate the presence of drug/polymer. The multilayered coatings of Dex-loaded TNTs was analyzed on a FTIR spectrometer (Model 6300, Bio-Rad, USA). Dex alone as well as gelatin and chitosan alone was used as a control.

Drug Release

Release of Dex from 30nm/Dex/(Gel/Chi)$_6$, 70nm/Dex/(Gel/Chi)$_6$, and 100nm/Dex/(Gel/Chi)$_6$ was investigated. Five samples of each group were immersed in 5ml of PBS (pH 7.4) at 37°C. After incubating for 3h, 6h, 12h, 24h, 48h, 72h, 96h, 120, 144, 168h, 240h, and 336h, 500μl of the solution was aliquotted to determine the amount of drug released by a UV spectrophotometer (Cary 500 scan UV–vis–NIR) at 242nm, and the same volume of fresh PBS solution was added.[28,29] The corresponding Dex concentration was calculated according to the standard calibration curve for Dex, and the amount of Dex in each sample was divided by the total number of samples. The accumulative Dex release rate (%) was calculated following the equation: Dex (%) = (total amount of Dex release in each sample)/(total amount of Dex initial loading in each sample) × 100%. All samples were studied in triplicate.

70nm/Dex/(Gel/Chi)$_6$ was chosen to observe the degradation of the Gel/Chi multilayered coating. First, rMSCs were seeded on the surface of the fabricated 70nm/Dex/(Gel/Chi)$_6$ sample at an initial density of 5×10^2/cm^2. After culture at 37°C for 24h, the degradation of the Gel/Chi multilayered coating was observed by SEM.

Isolation and culture of rMSCs

rMSCs were isolated and purified from 3-4 week old Sprague-Dawley rats according to the methods from a previous study.[30] All procedures performed in this study were in accordance with an IACUC approved protocol of Chongqing Medical University. Briefly, two 4-week old female Sprague-Dawley rats were euthanatized with 10% chloral hydrate. Then, femurs and tibias were harvested aseptically and soaked in ice-chilled PBS, and then quickly transferred to a dish containing DMEM/F12 (Hyclone, China) supplemented with 10% FBS (Gibco, USA), 100U penicillin (Invitrogen, USA), and 100μg/ml streptomycin (Invitrogen, USA) in a biosafety cabinet. The two ends of each bone were cut off with a scissor, and the marrow was flushed out from both sides of the bone thoroughly and then suspended with a sterilized syringe. Subsequently, the cell suspension was filtered through a 70μm nylon strainer to remove blood aggregates and bone debris and then cultured in DMEM/F12 supplemented with 10% FBS (Gibco, USA), 100U penicillin (Invitrogen, USA), 100μg/ml streptomycin (Invitrogen, USA), and 12μM L-glutamine (Invitrogen, USA) in 5% CO2 at 37°C. The cell culture medium was replaced every 2-3 days. When reaching confluence, cells were detached by incubating with 0.25% trypsin/EDTA for 2 min at 37°C, centrifuged, and resuspended in fresh medium for reseeding 1:2 in new culture flasks. The passaged cells were orderly denoted by passage (P) as P1, P2, P3, etc. All experiments used rMSCs from P3 in this study.

Cytoskeleton observation

rMSCs were seeded onto smooth Ti (control group), 30nm/Dex/(Gel/Chi)$_6$, 70nm/Dex/(Gel/Chi)$_6$, and 100nm/Dex/(Gel/Chi)$_6$ substrates which were previously sterilized under ultraviolet light in a biological hood for 1h, at an initial density of 8×10^3 cells/cm^2. The cell cytoskeleton was stained after 24h of culture according to the following steps. First, rMSCs adhered to different substrates were fixed with 4% paraformaldehyde at room temperature for 30 min. Then, the fixed samples were washed 3 times with PBS and treated with 0.2% Triton X-100 at 4°C for 10min. rMSCs were then stained with 5U/ml rhodamine-phalloidin (Invitrogen Co., USA) at 4°C for 12h. Subsequently, the nuclei of the cells were stained with 300ng/ml DAPI (Invitrogen Co., USA) at 4°C for 20 min. Finally, the samples were sealed with 95% glycerin. The cytoskeleton and nuclei of rMSCs on different substrates were visualized and photographed by confocal laser scanning microscopy (CLSM; TCS SP8, Leica, Germany).

Cell morphologies from SEM observations

rMSCs were seeded onto smooth Ti (control group), 30nm/Dex/(Gel/Chi)$_6$, 70nm/Dex/(Gel/Chi)$_6$, and 100nm/Dex/(Gel/Chi)$_6$ substrates which were previously sterilized under ultraviolet light in a biological hood for 1h, at an initial density of 5×10^3/cm^2. After culturing for 24h, the samples were washed 3 times with PBS and fixed with 2.5% glutaraldehyde for 1h at room temperature, and then transferred to a 4°C freezer for 24h. Subsequently, the samples were rinsed 3 times with PBS, and then 50%, 60%, 70%, 80%, 90%, and 100% ethanol was used to graded dehydrate for 10 minutes each; 100% ethanol was repeated for another two times. Then, the liquid was removed and hexamethyldisilazane (HDMS) was added; the samples were evaporated overnight under the hood. After the samples were thoroughly dried, golden coating was performed. Finally, images were observed with SEM (FEINova 400 Nano SEM, Phillips Co, Holland).

Cell adherence assay

rMSCs were seeded onto smooth Ti (control group), Ti/Dex, Ti/Dex/(Gel/Chi)$_6$ 30nm/Dex/(Gel/Chi)$_6$, 70nm/Dex/(Gel/Chi)$_6$, and 100nm/Dex/(Gel/Chi)$_6$ substrates at an initial density of 2×10^5/cm^2 in 24 well plates. After culture for 1h, an MTT assay was applied to detect the cell adherence ability. Five replicates were analyzed in each group. After removing the medium and rinsing 3 times with PBS, the samples were transferred to fresh wells. Next, 1ml of DEME/F12 and 200μl of MTT solution (5mg/ml) were added into each well. The solution in the wells was discarded after the samples incubated at 37°C for 4h, and 1ml of dimethyl sulfoxide was then added into each well in order to dissolve the formazan crystals. The optical density (OD) of the resulting solution was determined at a wavelength of 570 nm.

Cell proliferation

rMSCs were seeded onto smooth Ti (control group), 30nm/Dex/(Gel/Chi)$_6$, 70nm/Dex/(Gel/Chi)$_6$, and 100nm/Dex/(Gel/Chi)$_6$ substrates at an initial density of 5×10^3/cm^2. After culture for 1 day, 3 days, and 7days, the MTT assay was employed to detect the cell proliferation ability in the manner described in section "Cell adherence assay". Five replicates of each group were measured as well.

Alkaline phosphatase activity assay

rMSCs were seeded onto different substrates at an initial density of 2×10^4/cm^2 in 24 well plates. After 3 days, 7 days, and 14 days of culture, the ALP activity of cells adhered to each sample was detected. Cells in each sample were lysed with 100 μl 1% Triton X-100 for three freeze-thaw cycles, and 30μl of the cell lysate was aliquotted to measure ALP activity with a spectrophotometric microplate reader (F039300, Tecan) at 405 nm following the manufacturer's instructions. Total intracellular protein content was determined with a BCA assay

kit (Beyotime institute of biotechnology, China), and the optical density was measured at 570 nm with a spectrophotometric microplate reader (F039300, Tecan) in each sample. The relative total intracellular protein synthesized by rMSCs was calculated based on a standard absorbance curve obtained from the known concentration of albumin. Finally, ALP activity was calculated according to the following equation: ALP activity (U/gprot) = (OD of test well - OD of blank well)/(OD of standard well - OD of blank well) × concentration of standard albumin solution (0.02mg/ml)/total intracellular protein of test sample (gprot/ml). Five replicates in each group were analyzed as well.

Mineralization

rMSCs were seeded onto smooth Ti (control group), 30nm/Dex/$(Gel/Chi)_6$, 70nm/Dex/$(Gel/Chi)_6$, and 100nm/Dex/$(Gel/Chi)_6$ substrates at an initial density of $2\times10^4/cm^2$. After 21 days culture, cells adhered to different substrates were stained by alizarin red S according to the methods of a previous study.[26] rMSCs were fixed in 2.5% glutaraldehyde for 30 min and then stained with 40 mM alizarin red S for another 20 min at room temperature. Then, the cells were rinsed 3 times with distilled water. Subsequently, 400μl of an acetic acid (10% v/v) solution was added each well and placed at room temperature for 30 min. Cells were then scraped from the substrate surface and transferred to a centrifuge tube. After suspension, the samples were heated at 85°C for 10 min and then centrifuged for 15 min. The supernatant was transferred to another fresh centrifuge tube and 200μl of 10% ammonium hydroxide was added to each sample. The absorbance of the reaction liquid was detected at 405 nm using a spectrophotometric microplate reader (F039300, Tecan). Five replicates in each group were analyzed as well.

Real-time PCR

rMSCs cultured on different substrates were analyzed after 7 days, 14 days, and 21 days culture with an initial density of $2\times10^4/cm^2$. RNA extraction, reverse transcription, and real-time PCR were performed according to the instructions of RNA extraction kit (Code No: 9108/9109, Takara, Japan), PrimeScript RT reagent kit with gDNA eraser (Code No: RR820A, Takara, Japan), and real-time PCR assay kit (Code: No.RR047A, Takara, Japan), respectively. Real-time PCR was performed with the Bio-Rad CFX Manager system (USA). The amplification was operated with cycling conditions of 95°C for 1 min, followed by 40 cycles of 95°C for 10s, 60°C for 40s, and melting curves were recorded during the 65°C to 95°C melting process with continual fluorescence data acquisition. The primers used in this study were as follows: Runx2: forward, 5'-CCGGTCTCCTTCCAGGAT-3'; reverse, 5'-GGGAGCTGCTGTGGCTTC-3';OSX:forward,5'-GGGAAAAGGAGGCACAAAGAA-3';reverse,5'-AGGAAATGAGTGGGGAAAGGG-3';GAPDH:forward,5'-CCTGGAGAAACCTGCCAAG-3';reverse,5'-CACAGGAGACAACCTGGTCC-3'. The target gene expression was normalized to a house-keeping gene, GAPDH. The experiment was repeated 3 times.

Statistical analysis

Data in all experiments were expressed as mean ± standard deviation (SD). The statistical analysis was determined with a one-way ANOVA and a Student's t-test performed with SPSS 19.0 at confidence level of 95%. The statistical charts were drawn with Graphpad Prism 5.

Results and discussion

Fabrication and multilayered coatings of TNTs

How to effectively improve the biocompatibility of titanium implants in order to accelerate the speed of osseointegration with better osteogenic response is still a tremendous challenge.[7,28] The fabrication of TNTs has been considered to be a preeminent approach to modify the titanium implant surface.[29] Titanium surfaces with TNTs are more advantageous for creating a suitable microenvironment for proliferation and osteogenic differentiation of MSCs compared with smooth titanium surfaces.[12, 31-32] In this study, TNTs of 30nm, 70nm, and 100nm diameter observed with SEM were successfully fabricated by anodization under potentials of 10v, 20v, and 30v, respectively. The TNT arrays of different diameters were of one dimension with no collapse, fragmentation, or desquamation of the nanotube layers, as shown in Fig1. (B, C and D). While the Ti sheet was relatively flat and smooth according to SEM observation (Fig1A), and there were some micro-rough structures on it.

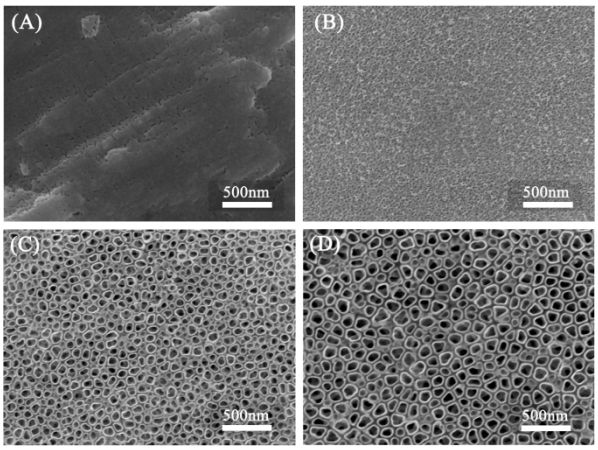

Fig.1 SEM of smooth Ti and 30nm, 70nm, and 100nm diameter TNTs (magnified 100000×). (A) smooth Ti, (B) 30nm diameter TNTs , (C) 70nm diameter TNTs, (D) 100nm diameter TNTs.

A chemical delivery system based on these nanotube structures was considered to speed wound healing and induce cells differentiation.[33,34] 30nm, 70nm, and 100nm in diameters TNTs were successfully constructed and served as nanovectors proved by our data in this paper. We hypothesized that one of the most efficient ways to achieve osteointegration could be local delivery of proper osteogenic drugs at the implant/tissue interface. Additionally, a sustained-release drug delivery system is vital for maintaining the bioactivity of the drugs, which enhances the curative effect. According to previous studies, Gel/Chi "lids" may help to improve the controlled release of a drug,[35] and are completely biodegradable.[21-23] Hence, to create a barrier for drug release in our study, Gel/Chi multilayered structures were layered on the TNTs (which had Dex previously loaded). Dex has been used as a model drug for loading the three types of diameters anodized nanotubes for its promoting osteogenesis properties. Fig2. (A and B) shows the SEM observation of TNTs coated with Gel/Chi multilayered

structures. No nanotubes were observed in SEM images, which indicated that the nanotubes were completely covered.

The chemical compositions of 70nm TNTs, 70nm/Dex and 70nm/Dex $(Gel/Chi)_6$ were measured by XRF, and the results are depicted in Table 1. When Dex was loaded onto the surface of TNTs, the chemical elements F and O increased while Ti decreased. When 6 cycles Gel and Chi were placed on the TNTs, the chemical composition percentage of Ti was 0. This also demonstrated that TNTs were fully covered by the multilayered coatings.

Table.1 Chemical compositions of TNTs and TNTs with Dex and Dex –loaded TNTs with multilayered Gel/Chi coatings measured by XRF.

Substrate	O%	Ti%	F%	Fe%	p%
TNT	68.5969	29.6018	1.7025	0.0653	0.0335
TNT/Dex	72.1092	25.5508	2.1013	0.0218	0.0169
TNT/Dex/$(Gel/Chi)_6$	99.8959	0	0.1034	0.0005	0.0002

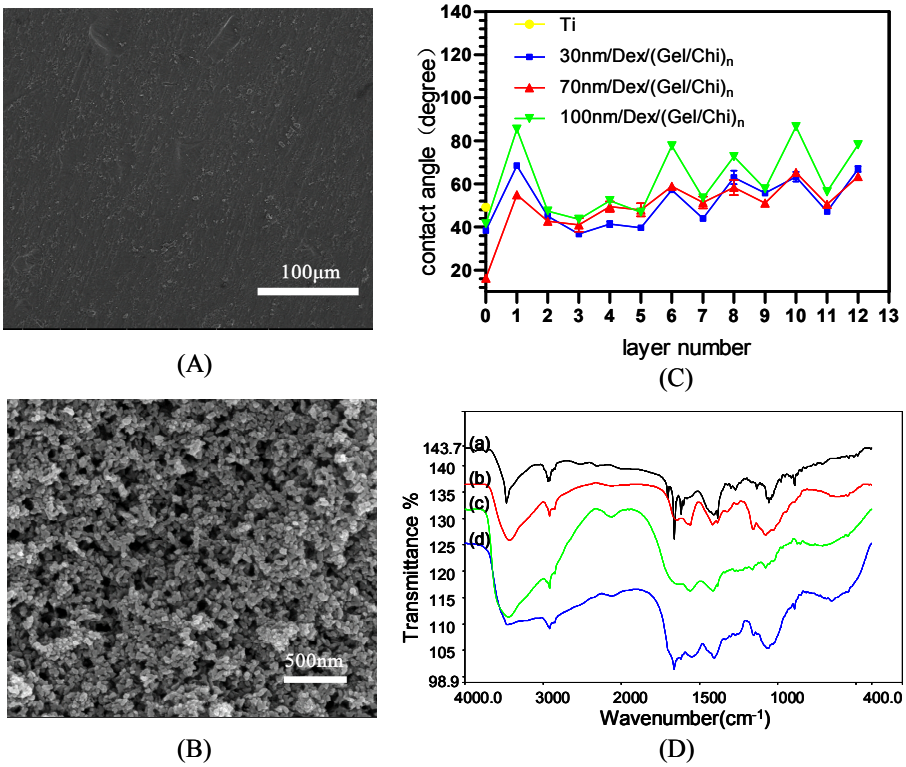

Fig.2 Surface characterization. (A) SEM of TNTs with multilayered Gel/Chi coatings, magnified 800×, (B) SEM of TNTs with multilayered Gel/Chi coatings, magnified 100000×. (C) Contact angles of smooth Ti and 30nm, 70nm, and 100nm TNTs with different layers of coatings. (D)FTIR spectra of native components and multilayered coatings: (a) dexamethasone alone (b) chitosan alone (c) gelatin alone (d) multilayered coatings of Dex –loaded TNTs.

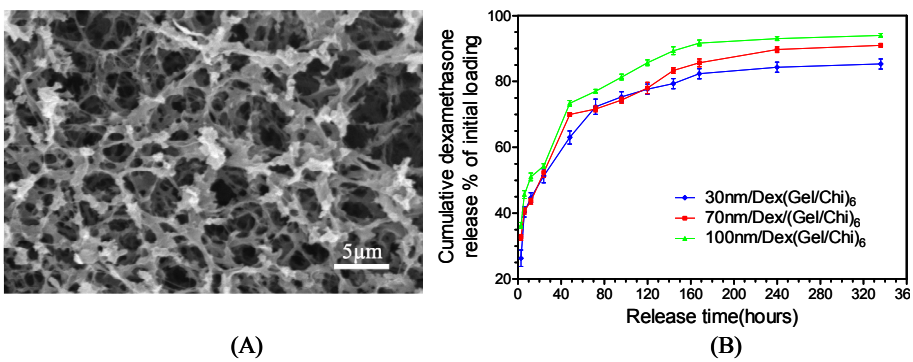

Fig.3 Drug Release. (A) SEM of the gradually degraded Gel/Chi multilayered coatings incubated at 37°C for 24h (magnified 2000×). (B) The cumulative Dex release profiles of 30nm/Dex/$(Gel/Chi)_6$, 70nm/Dex/$(Gel/Chi)_6$, and 100nm/Dex/$(Gel/Chi)_6$ substrates.

Fig2C shows the contact angle characteristics of the different samples. When Gel and Chi were layered on different diameter TNTs, the contact angles increased. From the beginning of the fifth layer, the contact angles of Dex-loaded TNTs of different diameter all demonstrated regular, alternately changing features between 36° and 87°. This, again demonstrated that TNTs were fully covered by the multilayered coatings.

The presence of drug/polymer composite was further verified by FTIR, and depicted in Fig2D.

Drug release

Fig3A shows an SEM image of the multilayered coating on a TiO_2 nanotube after rMSCs were seeded onto the substrate and incubated at 37°C for 24h. A 3-dimensional network structure had formed due to the degradation of the Gel/Chi multilayered structure, which once again demonstrated the biodegradability of the Gel/Chi. The release profile of Dex is depicted in Fig3B. There was an initial burst release of Dex in all 3 diameters of the Dex-loaded TNTs. Dex was slowly released between 6h and 168h. After 168h, which was deemed to be the turning point, Dex was scarcely released. The tendency of release patterns was similar among 30nm/Dex/$(Gel/Chi)_6$, 70nm/Dex/$(Gel/Chi)_6$, and 100nm/Dex/$(Gel/Chi)_6$. Overall, approximately 85% of the initially loaded Dex was released from 30nm/Dex/$(Gel/Chi)_6$, 91% from 70nm/Dex/$(Gel/Chi)_6$, and 94% from 100nm/Dex/$(Gel/Chi)_6$. The Dex was observed to be released in an initial burst followed by a sustained release in all the Dex-loaded TNTs, which was consistent with the results from earlier studies.[15,36,37] All these data demonstrated that each of the the fabricated Dex-loaded TNTs with Gel/Chi multilayered coatings was a successful sustained release system.

Cell morphology

To evaluate the biological effects of these Dex-loaded TNTs, cell morphologies of the adhered cells were investigated. From CLSM observations, the rMSCs adhered to smooth Ti displayed a spindle shape, with poorer cell spreading compared with the other groups (Fig4. [A1 and A2] vs Fig4. [B1, B2, C1, C2, D1 and D2]). In contrast, the rMSCs adhered to the Dex-loaded TNT substrates all displayed good cell spreading and clear cytoskeleton as shown in Fig4. (B1, B2, C1, C2, D1 and D2).

We applied SEM to depict cell morphologies according to the references.[38-40] The SEM images of rMSCs on Dex-loaded TNT substrates are shown in Fig4. (A3, B3, C3, and D3). Comparatively, rMSCs grown on the 30nm/Dex/$(Gel/Chi)_6$ substrate (Fig4. [B3]) exhibited more filopodia than those on smooth titanium (Fig4. [A3]), 70nm/Dex/$(Gel/Chi)_6$ (Fig4. [C3]), and 100nm/Dex/$(Gel/Chi)_6$ (Fig4. [D3]). rMSCs grown on smooth titanium (Fig4. [A3]) exhibited the fewest filopodia.

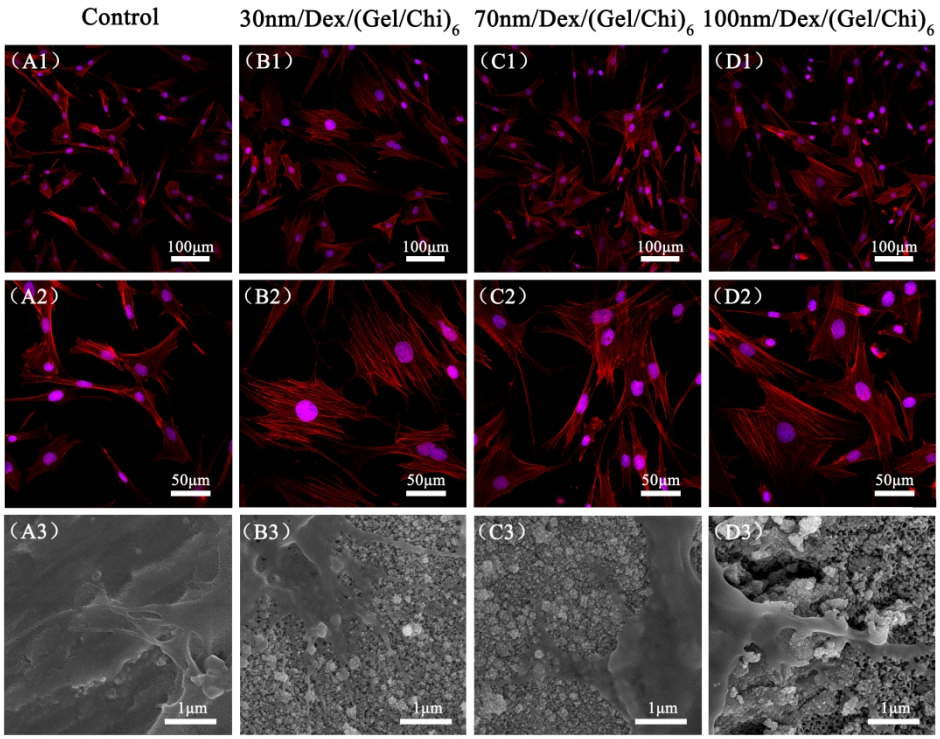

Fig.4 Cell morphologies of rMSCs seeded on different substrates after incubation for 24h. From CLSM observations (A1, A2) control group (smooth Ti), (B1, B2) 30nm/Dex/$(Gel/Chi)_6$, (C1, C2) 70nm/Dex/$(Gel/Chi)_6$, (D1, D2) 100nm/Dex/$(Gel/Chi)_6$.; From SEM observations (A3) control group (smooth Ti), (B3) 30nm/Dex/$(Gel/Chi)_6$, (C3) 70nm/Dex/$(Gel/Chi)_6$, (D3) 100nm/Dex/$(Gel/Chi)_6$.

CLSM and SEM demonstrated good cell spreading and filopodia formation on all the substrates. CLSM showed that rMSCs cultured on the three different Dex-loaded TNTs substrates displayed better cell spreading than on smooth titanium (Fig4. [B1, B2, C1, C2, D1 and D2] vs Fig4. [A1 and A2]), while there was no obvious difference in the three different diameter Dex-loaded TNTs substrates. Thus, we can conclude that Dex-loaded TNT substrates are more beneficial for cell spreading, which may be related to the composite functions of chemical stimulation from sustained released Dex and Gel/Chi. This is consistent with previous studies.[24, 41] SEM demonstrated that rMSCs on 30nm/Dex/$(Gel/Chi)_6$ had more cell filopodia compared with other groups (Fig4. [B3] vs Fig4. [A3, C3 and D3]). This may be related to the structures of

different diameter TNTs and chemical stimulation of sustained released Dex and Gel/Chi.

Cell adherence and proliferation

To further evaluate the biological effects of these Dex-loaded TNTs, cell adherence and proliferation were investigated. The MTT assay results shown in Fig5A depict the absorbance of formazan produced by rMSCs seeded onto control group (smooth Ti), Ti/Dex, Ti/Dex/$(Gel/Chi)_6$, 30nm/Dex/$(Gel/Chi)_6$, 70nm/Dex/$(Gel/Chi)_6$, and 100nm/Dex/$(Gel/Chi)_6$ after culture for 1h. According to the result, rMSCs on all diameters Dex-loaded TNTs substrates showed higher adhesion than those on smooth titanium ($P<0.05$). rMSCs cultured on 70nm/Dex/$(Gel/Chi)_6$ demonstrated the highest cell adherence ability ($P<0.05$).

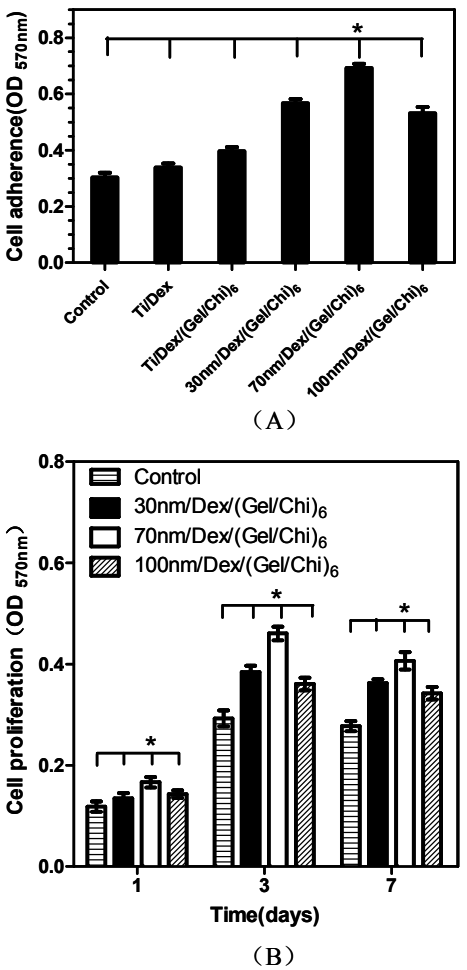

Fig.5 Cell adherence and proliferation. * represents $P<0.05$ compared with control group (smooth Ti), Ti/Dex, Ti/Dex/$(Gel/Chi)_6$, 30nm/Dex/$(Gel/Chi)_6$, and 100nm/Dex/$(Gel/Chi)_6$. (A) MTT assay of rMSCs seeded on control group (smooth Ti), Ti/Dex, Ti/Dex/$(Gel/Chi)_6$, 30nm/Dex/$(Gel/Chi)_6$, 70nm/Dex/$(Gel/Chi)_6$, and 100nm/Dex/$(Gel/Chi)_6$ after 1h culture at an initial density of $2\times10^5/cm^2$; (B) MTT assay of rMSCs cultured on control group (smooth Ti), 30nm/Dex/$(Gel/Chi)_6$, 70nm/Dex/$(Gel/Chi)_6$, and 100nm/Dex/$(Gel/Chi)_6$ after incubation for 1 day, 3 days, and 7 days at an initial density of $5\times10^3/cm^2$.

In addition, the MTT assay result shown in Fig5B depict the absorbance of formazan produced by rMSCs seeded onto different substrates after culture for 1 day, 3 days, and 7 days. rMSCs on 70nm/Dex/$(Gel/Chi)_6$ substrates showed higher proliferation abilities compared with other groups ($P<0.05$), and those on smooth titanium showed the lowest of all groups ($P<0.05$).

Dex-loaded TNTs were more beneficial for cell adhesion and proliferation than smooth titanium, possibly due to the function of the composite function of TNTs, Dex and Gel/Chi. Bauer et al demonstrated that cell adherence was affected by hydrophily, and cells had stronger adherence abilities on more hydrophilic surfaces.[42] An interesting phenomenon arose in this study. rMSCs showed stronger adherence abilities on Dex-loaded TNTs, which were less hydrophilic than the smooth titanium. Therefore, we could conclude that it is not only hydrophily that affects cell adherence and proliferation, but other factors, such as chemical composition and material structure may also play a vital role. This conclusion is consistent with that of a previous study.[14]

Cell osteogenic differentiation

In order to further evaluate the biological effects of these Dex-loaded TNTs, osteogenic differentiation of the adhered rMSCs were investigated, including ALP activity, mineralization and gene expression of Runx2 and OSX.

Fig6A shows the ALP activity test results. rMSCs on all substrates demonstrated the same changing ALP activity tendencies: first rising, then falling, and finally reaching the highest level after 7 days of culture. rMSCs adhered to 30nm/Dex/$(Gel/Chi)_6$ substrates showed the highest ALP activity ($P<0.05$) after 7 days culture, while those on smooth titanium showed the lowest ($P<0.05$). Mineralization was tested after 21 days of culture (Fig6B). rMSCs grown on Dex-loaded TNTs substrates displayed higher mineralization abilities than those on smooth titanium ($P<0.05$). rMSCs cultured on the 30nm/Dex/$(Gel/Chi)_6$ substrate also displayed higher mineralization abilities than those on other substrates ($P<0.05$). After culture for 7 days and 14 days, rMSCs grown on 30nm/Dex/$(Gel/Chi)_6$ substrates displayed the highest gene expression of both Runx2 and OSX, and rMSCs cultured on smooth titanium had lowest gene expression of both Runx2 and OSX. After 21 days of culture, rMSCs grown on 30nm/Dex/$(Gel/Chi)_6$ substrates displayed the highest gene expression of OSX ($P<0.05$), and rMSCs grown on smooth titanium had the lowest gene expression of OSX ($P<0.05$). rMSCs cultured on 30nm/Dex/$(Gel/Chi)_6$ and 70nm/Dex/$(Gel/Chi)_6$ substrates displayed similar gene expression of Runx2.

The ALP activity, mineralization, and mRNA expression of OSX and Runx2 on all the three types of Dex-loaded TNTs were remarkably higher than those on smooth titanium. This indicated that Dex-loaded TNTs were beneficial for rMSCs osteoblast differentiation. The composite structures of TNTs, Dex, and Gel/Chi promoted the osteoblasts differentiation of rMSCs. Accumulating evidence has demonstrated that Dex can mediate the expression of osteogenic markers such as ALP and the osteoblast-related gene Runx2, which promoted differentiation of MSCs.[19, 43] In this study, multilayered coatings of Gel/Chi pairs acted as a barrier to slow release Dex, which adhered rMSCs and induced osteoblast differentiation in a sustained manner. A similar phenomenon arose during the ALP activity test, mineralization, and real-time PCR analysis. rMSCs cultured on 30nm/Dex/$(Gel/Chi)_6$ substrates showed superiority over 70nm/Dex/$(Gel/Chi)_6$ substrates and 100nm/Dex/$(Gel/Chi)_6$ substrates in differentiating towards

osteoblasts, which may have been due to the higher amount of Dex preserved in 30nm/Dex/$(Gel/Chi)_6$[19] and the advantage of 30nm diameter TiO_2 nanotubes in promoting rMSC osteogenic differentiation.[44,45] Taken together, we conclude that Dex-loaded TNTs were beneficial for inducing rMSC osteoblast differentiation in vitro, and the composite function of TNTs, Dex and Gel/Chi promoted rMSCs osteoblast differentiation.

This study analyzed the functions of the composite structures of TNTs, Dex and Gel/Chi in rMSCs adherence, proliferation, and osteogenic differentiation. The separate functions of each should be further studied.

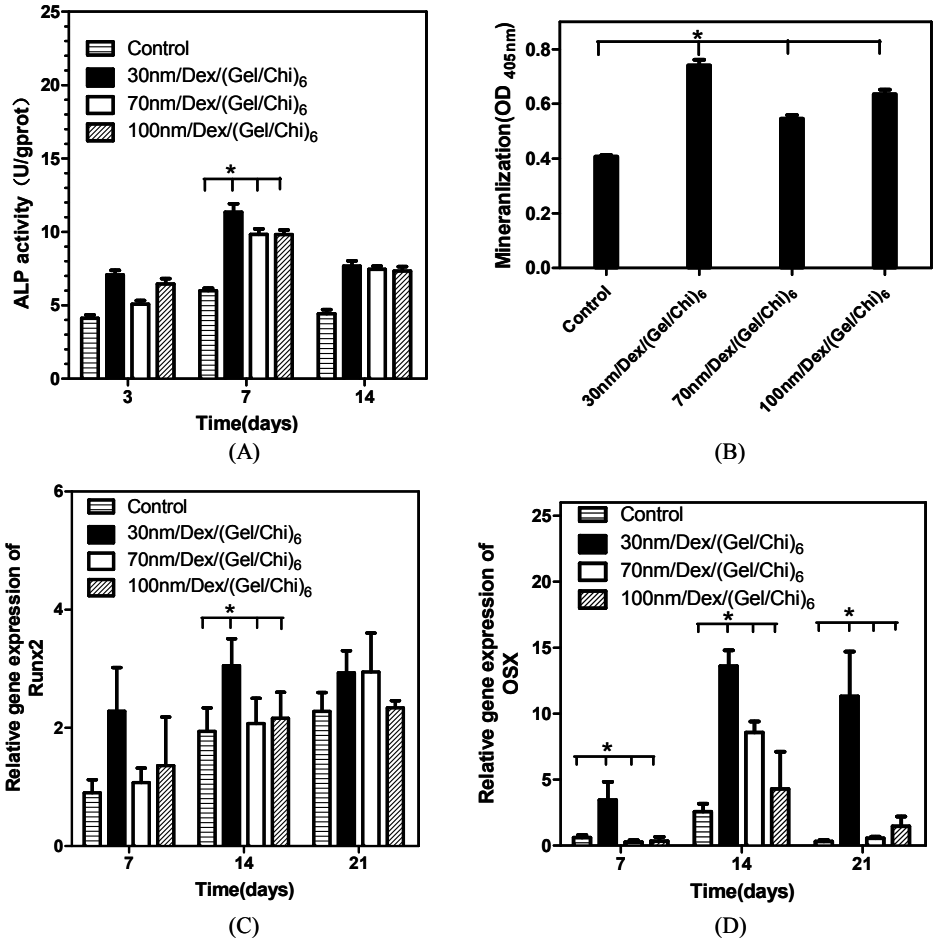

Fig.6 Cell differentiation of rMSCs cultured on control group (smooth Ti), 30nm/Dex/$(Gel/Chi)_6$,70nm/Dex/$(Gel/Chi)_6$,and100nm/Dex/$(Gel/Chi)_6$ at an initial density of $2\times10^4/cm^2$. * represents $P<0.05$ compared with control group (smooth Ti), 70nm/Dex/$(Gel/Chi)_6$, and 100nm/Dex/$(Gel/Chi)_6$. (A) ALP activity; (B) Quantitative mineralization; (C) Realtive gene expression of Runx2; (D) Relative gene expression of OSX.

Conclusions

In this study, Dex-loaded TNTs were fabricated to mimic implant surfaces, which employed TNTs on the surface of titanium substrates as drug nanoreservoirs to load Dex and Gel/Chi multilayers as efficient coverage for controlled release. Dex-loaded TNT substrates promoted adhesion, proliferation, and osteoblastic differentiation of rMSCs. This method may have potential value in the future for manufacturing implant biomaterials.

Acknowledgments

The work was financially supported by the Doctoral Startup Fund of the College of Stomatology in CMU (2011), Chongqing Municipal Health Bureau (2012-2-121), Chongqing Science & Technology Commission (cstc2012jjA0178), and the Specialized Research Fund for the Doctoral Program of China (SRFDP20125503120009), and Project Supported by Program for Innovation Team Building at Institutions of Higher Education in Chongqing in 2013.

Notes and references

1. J. Shi, A.R. Votruba, O.C.Farokhzad and R. Langer, *Nano Letters*, 2010, **10**, 3223.
2. A .Mamalis and S. Silvestros, *Journal of Oral Implantology*, 2013, **39**, 591.
3. A. Mellado-Valero, P. Buitrago-Vera, M.F. Solá-Ruiz and J.C. Ferrer-García, *Medicina Oral, Patologia Oraly Cirugia Bucal*, 2013, **18**, e869.

4. L. Zhao, S. Mei , P.K. Chu, Y. Zhang and Z.Wu, *Biomaterials*, 2010, **31**, 5072.
5. M. Sato, M.A. Sambito, A. Aslani, N.M. Kalkhoran, E.B. Slamovich and T.J. Webster, *Biomaterials*, 2006, **27**, 2358.
6. J.Y. Rho, L. Kuhn-Spearing and P. Zioupos, *Medical Engineering & Physics*, 1998, **20**, 92.
7. K.C. Popat, L. Leoni, C.A. Grimes and T.A. Desai, *Biomaterials*, 2007, **28**, 3188.
8. S. Oh, K.S. Brammer, Y.S. Li, D. Teng, A.J. Engler, S. Chien and S. Jin, *Proceedings of the National Academy of Sciences*, 2009, **106**, 2130.
9. W. Yu, J. Qiu and F. Zhang, *Colloids and surfaces B: Biointerfaces*, 2011, **84**, 400.
10. M.Y. Lan, C.P. Liu, H.H. Huang, J.K. Chang and S.W. Lee, *Nanoscale Research Letters*, 2013, **8**, 1.
11. N.M. Moore, N.J. Lin, N.D. Gallant and M.L. Becker, *Acta Biomaterialia*, 2011, **7**, 2091.
12. A.W. Tan, B. Pingguan-Murphy, R. Ahmad and S.A. Akbar, *Ceramics International*, 2012, **38**, 4421.
13. X.L. Liu, J. Lin and X.F. Chen, *RSC Advances*, 2013, **3**, 4885.
14. M. Lai, K. Cai, L. Zhao, X. Chen, Y. Hou and Z. Yang, *Biomacromolecules*, 2011, **12**, 1097.
15. Y. Hu, K.Y. Cai, Z. Luo, D.W. Xu, D.C. Xie, Y.R. Huang, W.H. Yang and P. Liu, *Acta Biomaterialia*, 2012, **8**, 439.
16. J. Shen, A.W. James, J.N. Zara, G. Asatrian, K. Khadarian, J.B. Zhang, S. Ho, H.J. Kim, K. Ting and C. Soo, *Tissue Engineering Part A*, 2013, **19**, 2390.
17. K. Cameron, P. Travers, C. Chander, T. Buckland, C. Campion and B. Noble, *Journal of Biomedical Materials Research Part A*, 2013, **101**, 13.
18. F. Langenbach and J. Handschel, *Stem Cell Research & Therapy*, 2013, **4**, 117.
19. Y. Su, Q. Su, W. Liu, M. Lim, J.R. Venugopal, X. Mo, S. Ramakrishna, S.S. Al-Deyab and M. El-Newehy, *Acta Biomaterialia*, 2012, **8**, 763.
20. J. S. Son, S.G. Kim, S.C. Jin, Z.G. Piao, S.Y. Lee, J.S.Oh, C.S. Kim, B.H. Kim and M.A. Jeong, *Biotechnology Letters*, 2012, **34**, 779.
21. S.T. Koshy, T.C. Ferrante, S .A. Lewin and D.J. Mooney, *Biomaterials*, 2014, **35**, 2477.
22. G. Gorczyca, R. Tylingo, P. Szweda, E. Augustin, M. Sadowska and S. Milewski, *Carbohydrate Polymers*, 2013, **102**, 901.
23. S.H. Hussein-Al-Ali, M.E. El Zowalaty, M.Z. Hussein, M. Ismail and T.J. Webste, *International Journal of Nanomedicine*. 2014, **9**, 549.
24. Y. Hu, K. Cai, Z Luo, L. Li, M.Lai, Y. Hou, Y. Huang, J .Li, X .Ding, B. Zhang and K.L. Sung, *Biomaterials*, 2012, **33**, 3515.
25. A. Mihic, J. Li, Y. Miyagi, M.Gagliardi, S.H. Li, J . Zu, R.D. Weisel, G. Keller and R.K. Li, *Biomaterials*, 2014, **35**, 2798.
26. B.P. Koppolu, S.G. Smith, S.Ravindranathan, S. Jayanthi, T.K. Suresh Kumar and D.A. Zaharoff, *Biomaterials*, 2014, **35**, 4382.
27. L. Peng, M.L. Eltgroth, T.J. LaTempa, C.A. Grimes and T.A. Desai, *Biomaterials*, 2009, **30**, 1268.
28. D.S. Kommireddy, S.M. Sriram, Y. M. Lvov and D.K. Mills, *Biomaterials*, 2006, **27**, 4296.
29. K. Shankar, G.K. Mor, H.E. Prakasam, S. Yoriya, M.Paulose, O.K. Varghese and C.A.Grimes, *Nanotechnology*, 2007, **18**, 065707.
30. L. Zhang and C. Chan, *Journal of Visualized Experiments*, 2010, **37**, 1.
31. S.C. Roy, M. Paulose and C. A. Grimes, *Biomaterials*, 2007, **28**, 4667.
32. K. S. Brammer, S. Oh, C.J. Cobb, L.M. Bjursten, H. Heyde and S. Jin, *Acta Biomaterialia*, 2009, **5**, 3215.
33. P.A. Baeuerle and V.R. Baichwal, *Advances in Immunology*, 1997, **65**, 111.
34. L. Sun and R. Guo, *Irish Journal of Medical Science*, 2013, **182**, 1.
35. S. Kona, J.F. Dong, Y. Liu, J. Tan and K.T. Nguyen, *International Journal of Pharmaceutics*, 2012, **423**, 516.
36. L. Leprince, A. Dogimont, D. Magnin and S. Demoustier-Champagne, *Journal of Materials Science: Materials in Medicine*, 2010, **21**, 925.
37. R. Wadhwa, C.F. Lagenaur and X.T. Cui, *Journal of Controlled Release*, 2006, **110**, 531.
38. W. C. Clem, S. Chowdhury, S. A. Catledge, J. J. Weimer, F. M. Shaikh, K. M. Hennessy, V. V. Konovalov, M. R. Hill, A. Waterfeld, S. L. Bellis and Y. K. Vohra, *Biomaterials*, 2008, **29**, 3461.
39. W.Q. Yu, X.Q. Jiang, L. Xu, Y.F. Zhao, F.Q. Zhang and X. Cao, *J Biomed Mater Res Part B*, 2011, **99B**, 207.
40. K. S. Brammer, S. Oh, C.J. Cobb, L.M. Bjursten, H. Heyde and S. Jin, *Acta Biomaterialia*, 2009, **5**, 3215.
41. K. Cameron, P.Travers, C. Chander, T. Buckland, C. Campion and B. Noble, *Journal of Biomedical Materials Research Part A*, 2013, **101**, 13.
42. S.Bauer, J.Park, K. von der Mark and P. Schmuki, *Acta Biomaterialia*, 2008, **4**, 1576.
43. C.D. Hoemann, H. El-Gabalawy and M.D.McKee, *Pathologie Biologie*, 2009, **57**, 318.
44. J.M. Oliveira, N. Kotobuki, M. Tadokoro, M. Hirose, J.F. Mano, R.L. Reis and H. Ohgushi, *Biomaterials*, 2009, **30**, 804.
45. J. Park, S. Bauer, K. von der Mark and P. Schmuki, *Nano Letters*, 2007, **7**, 1686.